Computers in Biology and Medicine 42 (2012) 319–327

Contents lists available at ScienceDirect

Computers in Biology and Medicine

journal homepage: www.elsevier.com/locate/cbm

Classifying cardiac biosignals using ordinal pattern statistics and symbolic dynamics

U. Parlitz [a,b,*], S. Berg [c], S. Luther [a,b,d], A. Schirdewan [e], J. Kurths [f,g], N. Wessel [f]

[a] Max Planck Institute for Dynamics and Self-Organization, Am Fassberg 17, 37077 Göttingen, Germany
[b] Institute for Nonlinear Dynamics, Georg-August-Universität Göttingen, Am Fassberg 17, 37077 Göttingen, Germany
[c] Drittes Physikalisches Institut, Georg-August-Universität Göttingen, 37077 Göttingen, Germany
[d] Department of Biomedical Sciences, Cornell University, Ithaca, NY, 14853, USA
[e] Department of Cardiology and Pneumology, Charité-Universitätsmedizin Berlin,Campus Benjamin Franklin, Hindenburgdamm 30, 12203 Berlin, Germany
[f] AG Nichtlineare Dynamik (S) / Kardiovaskuläre Physik, Institut für Physik, Humboldt-Universität zu Berlin, Robert-Koch-Platz 4, 10115 Berlin, Germany
[g] Potsdam Institute for Climate Impact Research, Telegrafenberg A3114473 Potsdam, Germany

ARTICLE INFO

Keywords:
ECG classification
Heart rate variability
Ordinal pattern statistics
Permutation index
Symbolic dynamics

ABSTRACT

The performance of (bio-)signal classification strongly depends on the choice of suitable features (also called parameters or biomarkers). In this article we evaluate the discriminative power of ordinal pattern statistics and symbolic dynamics in comparison with established heart rate variability parameters applied to beat-to-beat intervals. As an illustrative example we distinguish patients suffering from congestive heart failure from a (healthy) control group using beat-to-beat time series. We assess the discriminative power of individual features as well as pairs of features. These comparisons show that ordinal patterns sampled with an additional time lag are promising features for efficient classification.

1. Introduction

Heart rate variability reflects the complex interaction of control loops of the cardiovascular system and its nonlinear response to perturbations. Cardiac diseases often manifest themselves in characteristic changes in the heart rate variability and in the corresponding patterns of beat-to-beat intervals (BBI). Consequently, the ability to classify (or: distinguish between) physiological and pathological BBI patterns is critically important for the development of new diagnostic tools. Successful classification of time series of beat-to-beat intervals, however, strongly depends on the availability of significant features [1–10]. In the following we shall introduce a new family of features based on ordinal pattern statistics. We compare these new features with conventional heart rate variability (HRV) parameters [1] as well as features based on symbolic dynamics [4–6]. The performance of these three classes of features will be evaluated and compared using BBI time series from a (healthy) control group and patients suffering from congestive heart failure (CHF).

2. Features

In this section we shall briefly introduce features deduced from heart rate variability parameters, symbolic dynamics, and ordinal pattern statistics.

2.1. Heart rate variability parameters

Standard methods of HRV analysis [1] include time and frequency domain parameters. Time domain parameters are based on statistical methods derived from the RR-intervals as well as the differences between them. The mean heart rate (meanNN) is the simplest parameter, while the standard deviation for the whole time series (sdNN) is the most prominent HRV measure for estimating overall HRV. A list of commonly used parameters is given in Table 1. These parameters can be calculated for short (5 min) and long (24 h) term epochs, representing short-term and long-term variability, respectively.

Frequency domain HRV parameters focus on periodic components in the heart rate time series [11]. There are different techniques for spectral analysis: methods based on the fast Fourier transform (FFT), parametric autoregressive modelling, or wavelet decompositions. Very low, low and high frequencies (see Table 1) can be estimated from 5 min ECG recordings. The high frequency power reflects modulation of vagal activity by respiration, whereas the low frequency power represents vagal

* Corresponding author at: Max Planck Institute for Dynamics and Self-Organization, Am Fassberg 17, 37077 Göttingen, Germany. Tel.: +49 551 5176 369.
E-mail address: ulrich.parlitz@ds.mpg.de (U. Parlitz).

0010-4825/$ - see front matter © 2011 Elsevier Ltd. All rights reserved.
doi:10.1016/j.compbiomed.2011.03.017

Table 1
Description of time- and frequency domain HRV parameters. BBI stands for (filtered) beat-to-beat intervals (NN-intervals).

Variable	Units	Definition
Time domain statistical methods		
meanNN	ms	Mean BBI (inversely related to mean heart rate)
sdNN	ms	Standard deviation of all BBI values
sdaNN5	ms	Standard deviation of successive five minutes BBI averages
cvNN	*none*	Coefficient of variation: sdNN/meanNN; quantifies long-range variabilities
rmssd	ms	Root mean square of successive BBI differences
pNN50	%	Percentage of NN-interval differences greater than 50 ms; quantifies short-range variabilities
pNNX	%	Percentage of beat-to-beat differences greater than *Xms* (e.g. $X=100/200$ ms)
pNNlX	%	Percentage of beat-to-beat differences lower than *Xms* (e.g. $X=10/20/30$ ms)
shannon	*none*	Shannon entropy of the histogram (density distribution of the BBI values)
renyiX	*none*	Renyi entropy of order X of the histogram (e.g. $X=2/4/0.25$)
Frequency domain methods		
P	ms^2	Total power from 0 to 0.4 Hz
ULF	ms^2	Ultra low frequency band 0–0.0033 Hz
VLF	ms^2	Very low frequency band 0.0033–0.04 Hz
LF	ms^2	Low frequency band 0.04–0.15 Hz
HF	ms^2	High frequency band 0.15–0.4 Hz
LF/HF	*none*	Quotient of LF and HF
LFn	*none*	Normalized low frequency band (LF/(LF+HF))

and sympathetic activity via the baroreflex loop. The low-to-high frequency ratio is used as an index of sympathovagal balance [12].

2.2. Symbolic dynamics

Symbolic dynamics provides a class of features by transforming the time series $x_1,x_2,\ldots,x_N$ into a sequence of symbols $s_1,s_2,\ldots,s_N$ from a finite alphabet. This sequence may be characterized statistically [5–10].

Notably, already two to four symbols result in an efficient characterization of beat-to-beat time series. For example, a symbolic description with two symbols was introduced in [6] using the symbols "0" and "1" to indicate differences of interbeat intervals below or above a threshold, i.e.

$$s_n(x_n)=\begin{cases}0: & |x_n-x_{n-1}|<\Delta\text{ms}\\ 1: & |x_n-x_{n-1}|\geq\Delta\text{ms},\end{cases} \tag{1}$$

where Δms indicates the time interval. A particular feature based on this kind of symbol sequences is POLVAR Δ that equals the probability of occurrence of the subsequence "000000" in the symbolic string and thus quantifies the low variability epochs. In our comparison of features we considered POLVAR5, POLVAR10 and POLVAR20.

Another study using only two symbols was presented by Cysarz et al. [7], who characterized HRV on short time scales by the symbolic sequence

$$s_n=\begin{cases}0 & \text{if} \quad \Delta RR_n\geq 0\\ 1 & \text{if} \quad \Delta RR_n<0,\end{cases} \tag{2}$$

where $\Delta RR_n=RR_n-RR_{n-1}$ denotes the difference of RR intervals and the symbols "0" and "1" represent deceleration and acceleration of heart rate, respectively.

Symbolic dynamics based on uniform quantization resulting in more than two symbols was used by Porta et al. [8,9] to compute information theoretic quantities. These quantities were shown to be quite efficient when used for characterizing short term heart period variability of CHF patients.

A symbolic dynamics representation of BBI time series using four symbols and non-uniform quantization levels was introduced by Wessel et al. [5,6] and is given by

$$s_n(x_n)=\begin{cases}0: & \mu<x_n\leq(1+a)\mu\\ 1: & (1+a)\mu<x_n<\infty\\ 2: & (1-a)\mu<x_n\leq\mu\\ 3: & 0<x_n\leq(1-a)\mu.\end{cases} \tag{3}$$

In Eq. (3), the transformation into symbols $s_n(x_n)$ is obtained using three non-uniform quanitization levels, where μ denotes the mean beat-to-beatinterval and a is a parameter that we have chosen to be equal to 0.05.

There are several quantities that characterize the resulting symbol strings. In this study we analyze the frequency distribution of words of length $W=3$, i.e. substrings which consist of three symbols from the alphabet $A=\{0,1,2,3\}$, leading to maximal $4^W=64$ different words (or bins when estimating probabilities of occurrence). This is a trade-off between sufficient dynamical resolution and adequate statistics to estimate the probability distribution.

A useful measure for decreased HRV is a high percentage of words consisting only of the symbols '0' and '2' (WPSUM02). Conversely, an indicator of increased HRV (WPSUM13) consists of a high percentage of all words which contain the symbols '1' and '3'.

Another measure of symbolic dynamics is the parameter WSDVAR, which measures the variability of the time series depending on a word sequence [10].

Based on symbolic representations and their probabilities of occurrence it is also possible to compute the Shannon entropy (FWSHANNON).

$$H(W)=-\sum_{k=1}^{4^W}p_k\log p_k \tag{4}$$

from the probabilities p_k of words. Large values of the Shannon entropy correspond to high complexity in the corresponding tachograms and vice versa.

Another feature that may be computed from the probability distribution of words is the number of forbidden words (FORBWORD) of length 3, i.e. the number of words which never or only seldomly occur. The larger the number of forbidden words, the more regular is the corresponding time series. If the time series is highly complex (in the sense of Shannon), only a few forbidden words will be found.

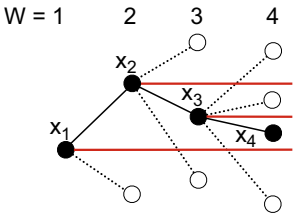

Fig. 1. Illustration of the construction principle of ordinal patterns of length W. For $W=2$ there are only two possible directions from x_1 to x_2, up or down. The third part of the pattern can be above x_2, below x_1 or between x_1 and x_2 as illustrated here. For pattern length $W=4$, there are four additional possible locations of x_4, leading finally to $W!$ different ordinal patterns.

A generalization of the Shannon entropy is the Renyi entropy of order q

$$H_q(W) = \frac{1}{1-q}\log\left(-\sum_{k=1}^{4^W} p_k^q\right) \tag{5}$$

that leads to the symbolic features FWRENYI025 ($q=0.25$) and FWRENYI4 ($q=4$). Again, higher values of these entropies indicate higher complexity in the corresponding tachograms.

2.3. Ordinal pattern statistics

Ordinal patterns [13–23] describe the relations within short segments of length W of a given time series. They are easy to compute and robust against noise. For this reason ordinal patterns have been used in a wide range of applications including the detection of determinism in noisy time series [18,19], estimation of transfer entropy in epilepsy [17], complexity analysis of time series [20], or classification [23].

The construction principle for ordinal patterns of length W is illustrated in Fig. 1. All possible ordinal pattern of subsequences of lengths $W=3$–5 are shown in Fig. 2. A unique index can be assigned to each ordinal pattern by interpreting the subsequence as a permutation that is characterized by a permutation index. This is done by first reordering the samples $x_n, x_{n+1}, x_{n+2}, \ldots x_{n+W-1}$ with respect to their amplitude such that $x_{\pi(n)} \le x_{\pi(n+1)} \le x_{\pi(n+2)} \le \cdots \le x_{\pi(n+W-1)}$ and then computing the permutation index of π. For example, a sequence $(x_n, x_{n+1}, x_{n+2}, x_{n+3}) = (2.22, 4.21, 1.30, 3.76)$ leads to a permutation (3, 1, 4, 2) with a permutation index of $I=11$ (see Fig. 2b). If two samples have the same amplitude, they are ordered with respect to time (i.e., $x_n = x_m$ yields (m,n) if $m < n$).[1] Note that some information about amplitudes and gradients or variability is lost upon this discretization. For example, a sequence 1, 1.01, 0.99 corresponds to the same permutation index $I=4$ as a sequence 1, 10 000, −20 000. Depending on the application any information about (absolute) amplitudes or derivatives has to be taken into account by other (additional) quantities or features.

Similar to the symbolic dynamics approach (Section 2.2) each time series can be transformed into a sequence of permutation indices that formally may also be considered as a sequence of symbols from a finite alphabet of size W! The concept of ordinal pattern can be extended [21,22] by considering not only consecutive samples but also subsequences with samples $x_n, x_{n+L}, x_{n+2L}, \ldots, x_{n+(W-1)L}$ that are separated in time by a lag of L sampling times T_S which corresponds to a delay of $T = L \cdot T_S$ in (absolute) time units. On this case $x(\_n+kL)$ is the RR interval at the beat $n+kL$. The probabilities of occurrence of specific patterns with permutation index I for a given delay T and length W are used as features for characterizing the underlying time series and will be denoted in the following by "perm(T, W, I)". The probability perm(T, W, I) will be given in percentage. Since the unit of time of beat-to-beat time series is "heart beats" in this case T is an integer number (= number of omitted beats + 1) that equals L. Furthermore, we compute the Shannon entropy based on all probabilities for a given delay T and a given word length W (in the following denoted as "perm entropy(T, W)").

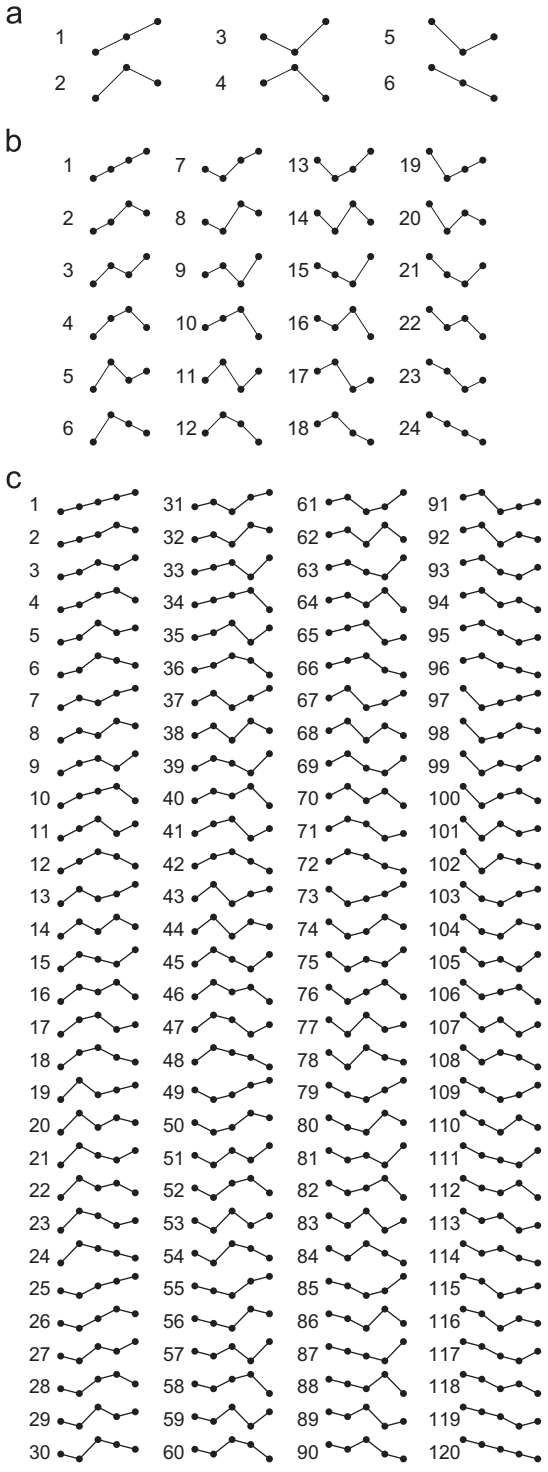

Fig. 2. Ordinal patterns of length (a) $W=3$, (b) $W=4$, (c) $W=5$ and corresponding permutation indices. For each pattern the values (or amplitudes) of the sequence are plotted vs. time (horizontal axis).

[1] If many pairs of equal samples occur in a time series, the ordering with respect to time will introduce a bias in the probability distributions and some random selection of (m,n) or (n,m) may be more appropriate.

Of course, in principle one could also consider even longer ordinal patterns ($W > 5$), but then very long time series are required to reliably estimate the fast growing number $W!$ of different patterns.

C-code for computing the permutation index can by found in Ref. [24]. Python or MATLAB (The MathWorks, Inc.) functions computing permutation indices from a time series for a given word length W and a time lag L are given in the Appendix.

3. Results

3.1. Data

To compare the performance of the three classes of features introduced in the previous section we applied them to two data sets describing long term beat-to-beat dynamics of patients suffering from congestive heart failure (CHF) and patients from a control group. The CHF data set consists of 24 h time series (sampling frequency 256 Hz) from 15 patients (11 male, 4 female, ages 56 ± 11 yr) available from Physionet [26] and beat-to-beat time series of 15 healthy elderly subjects (11 male, 4 female, ages 56 ± 5 yr) whose beat-to-beat time series (sampling frequency 128 Hz) were measured at Charité Berlin [25]. All CHF patients belonged to NYHA classes 3 and 4 [26].

The data have been preprocessed [4] to remove artifacts (e.g. double recognition, i.e. R-peak and T-wave recognized as two beats). Additionally, beats not originating from the sinus node of the heart, i.e. ventricular premature complexes (VPC), are removed. These beats are not directly controlled by the autonomous nervous system. About 6.8% of the samples of the CHF data and 3.3% of the control group samples were detected as artifacts A MATLAB implementation of the preprocessing algorithm is available from tocsy.pik-potsdam.de.

All features introduced in Section 2 were tested individually with respect to their ability to distinguish beat-to-beat time series of CHF patients from heartbeat data of healthy persons. Then, the most significant features of each group (Sections 2.1, 2.2, and 2.3) were selected to represent that class of features.

3.2. Classification results

Table 2.I shows mean values and standard deviations, as well as p-values [27] for the most important and most descriptive

Table 2
Significant features for CHF detection, including HRV parameters (I), symbolic dynamics (II), and ordinal patterns (III). Columns 2–4: Mean value ± standard deviation for the control group ('Control') and the CHF patients ('CHF') and p-values, Columns 5–7: Results of a Leave-One-Out Cross Validation test showing the percentage of correct classifications of data sets from the control group ("Control"), from the patient groups ("CHF"), and for all beat-to-beat time series ("Both").

	Feature	Mean value ± standard deviation		p-value	% of correct classifications		
		Control	CHF		Both	Control	CHF
I	VLF	7.8 ± 4.9	2.5 ± 4.1	2.7×10^{-05}	80	80	80
	LF	3.24 ± 2.34	0.55 ± 0.62	1.6×10^{-05}	70	73	67
	HF	0.90 ± 0.84	0.41 ± 0.50	4.3×10^{-03}	73	80	67
	P	54 ± 31	54 ± 157	3.4×10^{-05}	83	87	80
	LF/HF	4.20 ± 1.62	1.42 ± 0.73	1.3×10^{-06}	83	87	80
	LFn	0.79 ± 0.07	0.55 ± 0.12	1.3×10^{-06}	83	87	80
	meanNN	786 ± 60	668 ± 119	3.7×10^{-03}	77	93	60
	sdNN	121 ± 31.1	62 ± 24	3.5×10^{-06}	90	93	87
	cvNN	0.154 ± 0.036	0.093 ± 0.037	3.2×10^{-04}	80	87	73
	sdaNN1	114 ± 30	70 ± 61	9.0×10^{-05}	80	80	80
	rmssd	25.9 ± 9.9	20.1 ± 14.6	3.3×10^{-02}	73	87	60
	renyi2	2.96 ± 0.25	2.12 ± 0.40	1.5×10^{-07}	90	93	87
	renyi4	2.81 ± 0.27	1.97 ± 0.41	2.4×10^{-07}	87	87	87
	shannon	3.10 ± 0.24	2.33 ± 0.40	2.4×10^{-07}	87	87	87
II	FORBWORD	4.07 ± 4.27	0.87 ± 1.75	1.6×10^{-03}	80	87	73
	FWSHANNON	3.60 ± 0.15	3.83 ± 0.13	1.7×10^{-04}	80	73	87
	WPSUM02	0.057 ± 0.055	0.169 ± 0.072	1.1×10^{-04}	90	87	93
	WPSUM13	0.380 ± 0.105	0.203 ± 0.107	1.7×10^{-04}	83	87	80
	WSDVAR	2.25 ± 0.20	1.84 ± 0.24	7.1×10^{-05}	83	87	80
	POLVAR5	$6.9 \times 10^{-04} \pm 1.0 \times 10^{-03}$	0.036 ± 0.033	5.2×10^{-08}	93	93	93
	POLVAR20	0.286 ± 0.194	0.683 ± 0.216	1.1×10^{-04}	80	80	80
	PHVAR20	0.025 ± 0.029	0.013 ± 0.021	2.3×10^{-02}	53	60	47
	FWRENYI025	3.99 ± 0.06	4.07 ± 0.04	1.1×10^{-04}	73	67	80
III	perm(3,3,5)	13.8 ± 0.7	15.3 ± 0.6	1.6×10^{-05}	87	80	93
	perm(1,3,2)	11.3 ± 1.1	14.6 ± 1.9	2.7×10^{-05}	87	93	80
	perm(4,3,6)	18.6 ± 2.1	13.6 ± 3.0	2.7×10^{-05}	77	80	73
	perm(3,3,3)	12.3 ± 1.4	14.8 ± 1.1	3.4×10^{-05}	80	73	87
	perm(3,4,3)	2.89 ± 0.64	4.49 ± 0.52	1.3×10^{-08}	**100**	**100**	**100**
	perm(4,4,3)	2.76 ± 0.40	4.53 ± 0.80	3.9×10^{-07}	97	100	93
	perm(3,4,5)	2.87 ± 0.64	4.50 ± 0.66	1.3×10^{-06}	87	93	80
	perm(4,4,18)	5.57 ± 0.49	4.07 ± 0.89	1.8×10^{-06}	93	100	87
	perm(4,5,109)	1.34 ± 0.11	0.83 ± 0.20	9.0×10^{-08}	97	100	93
	perm(4,5,71)	1.16 ± 0.08	0.83 ± 0.14	9.0×10^{-08}	90	93	87
	perm(1,5,75)	0.17 ± 0.06	0.47 ± 0.20	9.0×10^{-08}	87	87	87
	perm(8,5,22)	0.85 ± 0.10	0.56 ± 0.09	1.5×10^{-07}	90	93	87

conventional HRV parameters (see Section 2.1). The best performance exhibits the standard deviation sdNN, the normalized low frequency band LFn, as well as the Shannon entropy (Eq. (4)) shannon and the Renyi Entropies (Eq. (5)) renyi2 and renyi4.[2]

Table 2.II shows classification results obtained with parameters from symbolic dynamics (see Section 2.2), where POLVAR5 provided best classification results.

The results for probabilities of ordinal patterns are shown in Table 2.III where we have listed those patterns that provided the best classification results (including several ordinal patterns of length $W=4$).

In Fig. 3 the p-values of the probabilities of permutations indices of subsequences sampled with lags T are plotted vs. T for different lengths W. For lags between 3 and 4 most of the p-values show local minima. These patterns span a period of $(W-1)T = 3\cdot 3-4\cdot 4 = 9-16$ heart beats, i.e. about 6–11 s (or 0.09–0.16 Hz) and they are correlated with the HRV parameters LF and LFn, which are known to have smaller values for CHF patients (due to medication or cardiac insufficiency) [28–30].

Therefore, we conjecture that ordinal patterns describing the dynamics on a time scale of about 0.09–0.16 Hz are quite sensitive and descriptive, because this is the frequency range, where BBI time series from CHF patients significantly differ from heart beats of healthy subjects.

3.3. Cross validation

Our second evaluation criterion is based on leave-one-out cross-validation (LOO-CV) of classification results obtained with individual features. For each feature a classifier was constructed by finding a threshold value that minimizes the total number of misclassifications in the training set. Then, the test data set was classified using this threshold. The classification were repeated for all possible separations into training and test sets and the percentage of correct classifications of test sets was computed. The results are given in columns 5–7 in Table 2 showing the percentage of correct classifications of data sets from the control group ("Control"), from the patient groups ("CHF"), and for all beat-to-beat time series ("Both"). As can be seen in Table 2.III feature perm(3,4,3) achieves 100% correct classifications in the LOO-CV test. An illustration of the corresponding ordinal pattern $I=3$ (see Fig. 2b) in terms of ECG-signals is shown in Fig. 4.

3.4. Unfiltered data

Table 3 shows results obtained from unfiltered CHF data and from unfiltered controls. Due to the robustness of ordinal pattern statistics their values differ not significantly from those estimated from the preprocessed data (cf. Table 2.III) and can be classified with the same leave-one-out cross validation. While some of the other parameters can be obtained from unfiltered data, most of them, however, show significantly reduced descriptive power, some even loose it entirely (e.g. P, sdNN, rmssd, or FORBWORD). The main cause for this failure may be beat-to-beat time series like the example shown in Fig. 5 that contain very long interbeat periods, probably due to interrupted measurements. If these very large (and spurious) BBI-values are not eliminated during a preprocessing or filtering process they may considerably distort parameters based on Fourier transforms or signal power. Notably, the statistics of ordinal patterns is almost unaffected by a few extreme amplitude values.

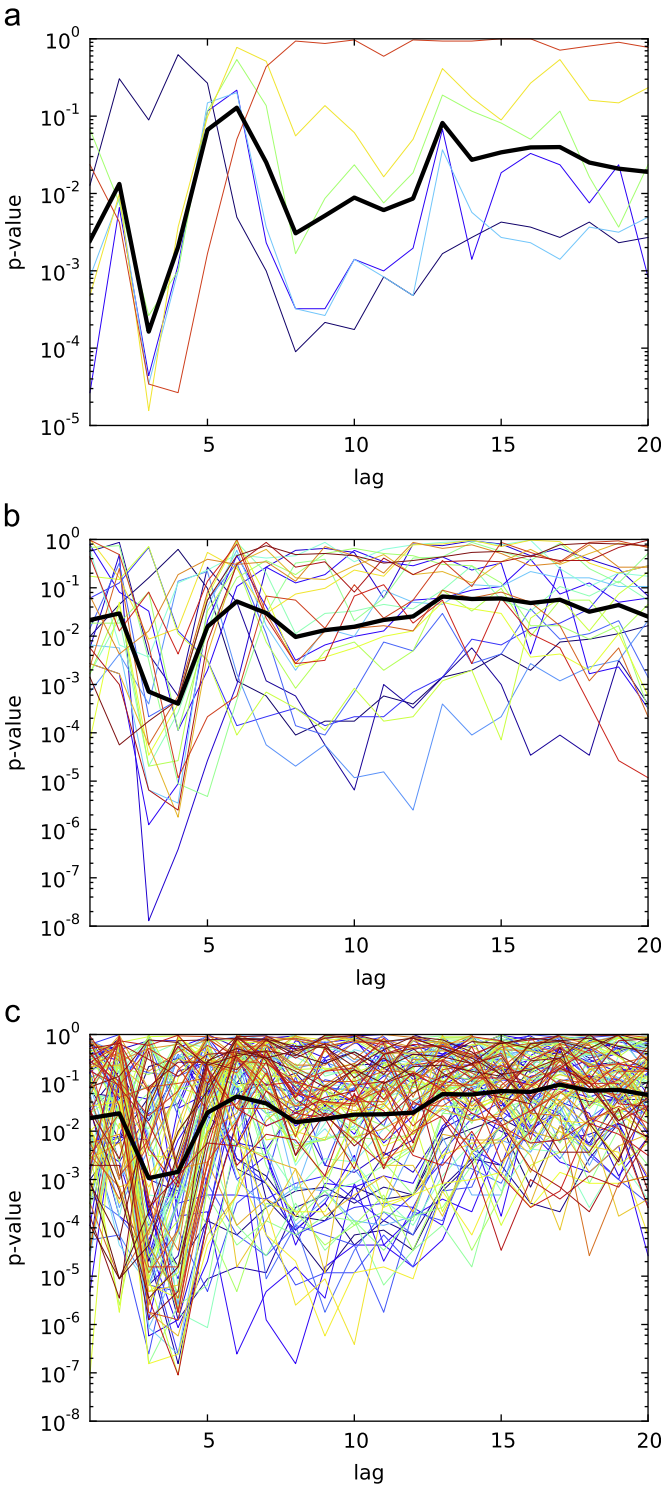

Fig. 3. p-values of the probabilities of permutations indices of subsequences sampled with lags T vs. lag T. (a) length $W=3$, (b) length $W=4$, (c) length $W=5$, The mean value of $\log(p)$-values is plotted as a thick (black) line with a clear minimum between lag 3 and 4.

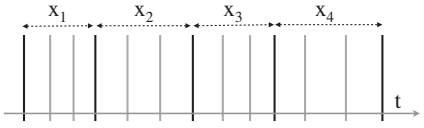

Fig. 4. Sketch of an ECG-signal (sequence of R-peaks) corresponding to an ordinal pattern perm(3,4,3). The time intervals x_k between every third beat ($T=3$) are ordered as $x_1 < x_3 < x_2 < x_4$.

[2] Bonferroni corrections were not explicitly applied but since most p-values listed here and in the following tables are very small, the results would remain significant even when including a correction factor of a few 100.

Table 3
Significant features for CHF detection based on unfiltered beat-to-beat time series (compare Table 2). Columns 2-4: Mean value ± standard deviation for the control group ('Control') and the CHF patients ('CHF') and *p*-values, Columns 5-7: Results of a Leave-One-Out Cross Validation test showing the percentage of correct classifications of data sets from the control group ("Control"), from the patient groups ("CHF"), and for all beat-to-beat time series ("Both").

	Feature	mean value ± standard deviation		*p*-value	% of correct classifications		
		Control	CHF		Both	Control	CHF
I	VLF	0.19 ± 0.11	187 ± 698	2.9×10^{-02}	67	80	53
	LF	0.084 ± 0.059	15.1 ± 56.2	2.2×10^{-01}	60	73	47
	HF	0.026 ± 0.022	2.22 ± 7.95	2.7×10^{-01}	70	100	40
	P	0.34 ± 0.20	247 ± 922	2.9×10^{-01}	63	73	53
	LF/HF	5.46 ± 2.61	1.30 ± 1.62	3.5×10^{-06}	87	87	87
	LFn	0.747 ± 0.077	0.386 ± 0.163	2.5×10^{-06}	93	93	93
	meanNN	802 ± 62	703 ± 155	1.5×10^{-02}	77	93	60
	sdNN	50 ± 15	210 ± 496	2.7×10^{-01}	67	87	47
	cvNN	0.063 ± 0.016	0.137 ± 0.232	4.1×10^{-01}	63	73	53
	sdaNN1	26.7 ± 6.6	183 ± 571	5.8×10^{-04}	80	87	73
	rmssd	30 ± 12	253 ± 598	1.4×10^{-01}	53	67	40
	renyi2	1.86 ± 0.31	1.21 ± 0.45	1.7×10^{-04}	80	80	80
	renyi4	1.69 ± 0.31	1.06 ± 0.40	1.1×10^{-04}	80	80	80
	shannon	2.06 ± 0.31	1.44 ± 0.49	1.7×10^{-04}	83	87	80
II	FORBWORD	29.2 ± 8.0	34.4 ± 8.9	1.3×10^{-01}	50	53	47
	FWSHANNON	2.64 ± 0.26	2.34 ± 0.36	3.2×10^{-03}	77	73	80
	WPSUM02	0.399 ± 0.135	0.633 ± 0.223	4.3×10^{-03}	80	87	73
	WPSUM13	0.327 ± 0.069	0.182 ± 0.146	1.4×10^{-03}	73	73	73
	WSDVAR	1.80 ± 0.23	1.17 ± 0.51	2.6×10^{-04}	80	87	73
	POLVAR5	$1.6 \times 10^{-03} \pm 2.2 \times 10^{-03}$	0.033 ± 0.033	1.3×10^{-06}	87	93	80
	POLVAR20	0.286 ± 0.194	0.648 ± 0.221	3.9×10^{-04}	77	80	73
	PHVAR20	0.029 ± 0.032	0.050 ± 0.115	1.1×10^{-01}	50	60	40
	FWRENYI025	3.42 ± 0.23	3.23 ± 0.29	2.9×10^{-02}	73	87	60
III	perm(3,3,5)	13.8 ± 0.7	15.4 ± 0.7	1.2×10^{-05}	87	80	93
	perm(1,3,2)	11.4 ± 1.2	15.8 ± 3.3	8.8×10^{-06}	87	93	80
	perm(4,3,6)	18.6 ± 2.1	13.5 ± 3.0	2.0×10^{-05}	87	80	93
	perm(3,3,3)	12.3 ± 1.4	14.7 ± 1.1	4.4×10^{-05}	80	73	87
	perm(3,4,3)	2.86 ± 0.64	4.48 ± 0.46	1.3×10^{-08}	100	100	100
	perm(4,4,3)	2.75 ± 0.38	4.47 ± 0.79	5.8×10^{-07}	97	100	93
	perm(3,4,5)	2.89 ± 0.63	4.65 ± 0.65	3.9×10^{-07}	90	93	87
	perm(4,4,18)	5.55 ± 0.46	3.89 ± 0.89	2.5×10^{-06}	97	100	93
	perm(4,5,109)	1.34 ± 0.11	0.82 ± 0.20	9.0×10^{-08}	97	100	93
	perm(4,5,71)	1.15 ± 0.09	0.83 ± 0.13	9.0×10^{-08}	97	100	93
	perm(1,5,75)	0.164 ± 0.056	0.411 ± 0.200	3.5×10^{-06}	87	87	87
	perm(8,5,22)	0.855 ± 0.095	0.561 ± 0.091	1.5×10^{-07}	93	93	93

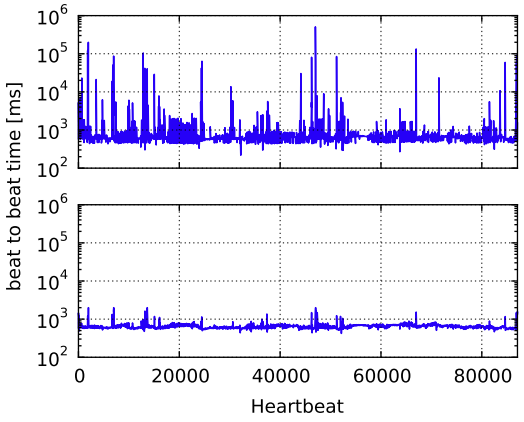

Fig. 5. Beat-to-beat time series containing very long (spurious) beat-to-beat intervals. Top: unfiltered data; bottom: filtered time series.

3.5. Separation of classes in two-dimensional feature spaces

In order to evaluate and compare the descriptive power of different types of features we shall consider now pairs of features that (individually) provided significant classification results. Fig. 6a shows a plot where for each (filtered) beat-to-beat time series (i.e. for each test person) the values of perm(3,4,3) are plotted vs. the corresponding probability perm(4,4,3). Both probabilities of ordinal patterns are normalized with respect to the smallest and the largest value occurring in the full data set. Points representing patients suffering from CHF are marked as a (red) cross while data associated with persons from the control group are plotted as filled (blue) circles. As can be seen, both sets of points are clearly separated. To quantify the amount of separation, a linear support vector machine [31] has been used to compute a separating line with a maximal margin.

Fig. 6(b) shows perm(3,4,3) vs. POLVAR5, and Fig. 6(c) perm(3,4,3) vs. renyi4. In all three diagrams shown in Fig. 6 feature perm(3,4,3) was used, because it exhibited perfect classification results in the leave-one-out cross-validation test (see Table 2 III) and enables a perfect separation already when used without any combination with some other feature.

To see whether two features that are individually not capable to separate both classes can indeed do so when being combined in a two-dimensional feature vector, Fig. 7 shows some examples of successful 2D-separation. Here different pairs of features provide

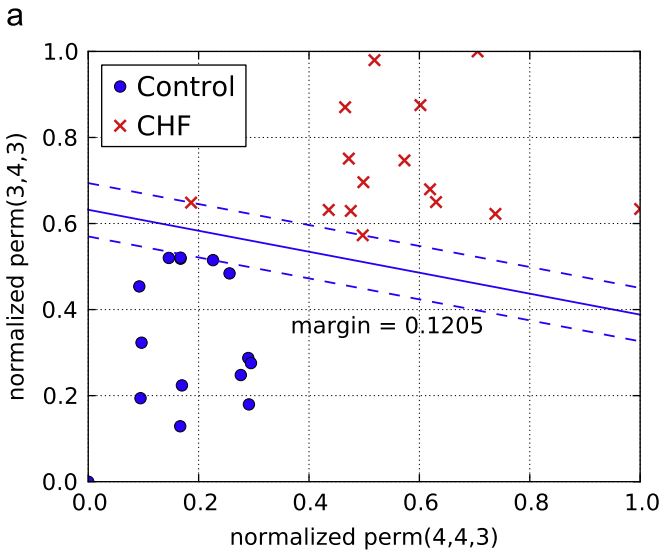

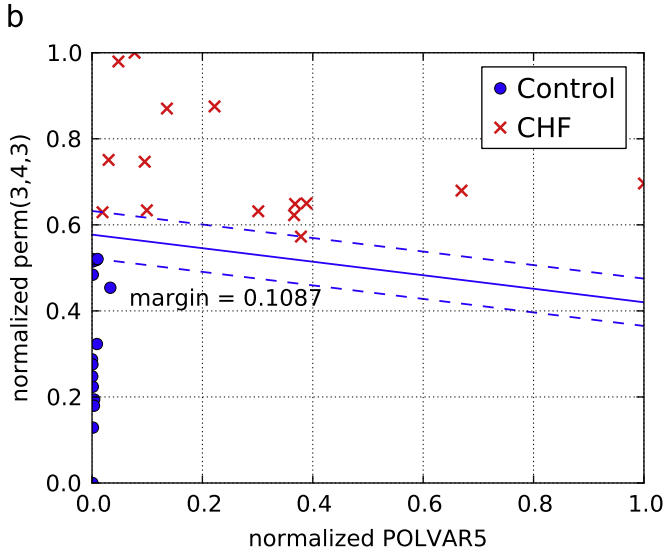

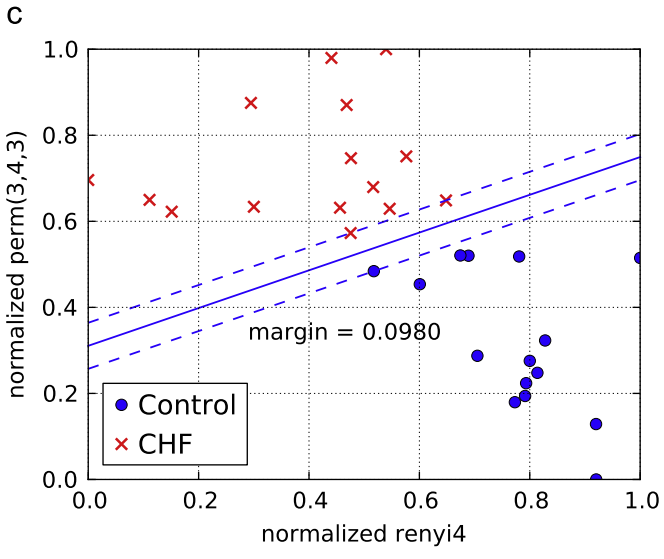

Fig. 6. Distribution of CHF cases (red crosses) and healthy subjects (blue filled circles) in two-dimensional feature spaces. The separating (solid) lines are computed using a linear support vector machine maximizing the margins (indicated by dashed lines). (a) perm(3,4,3) vs. perm(4,4,3), (b) perm(3,4,3) vs. POLVAR5, and (c) perm(3,4,3) vs. renyi4. (For interpretation of the references to color in this figure legend, the reader is referred to the web version of this article.)

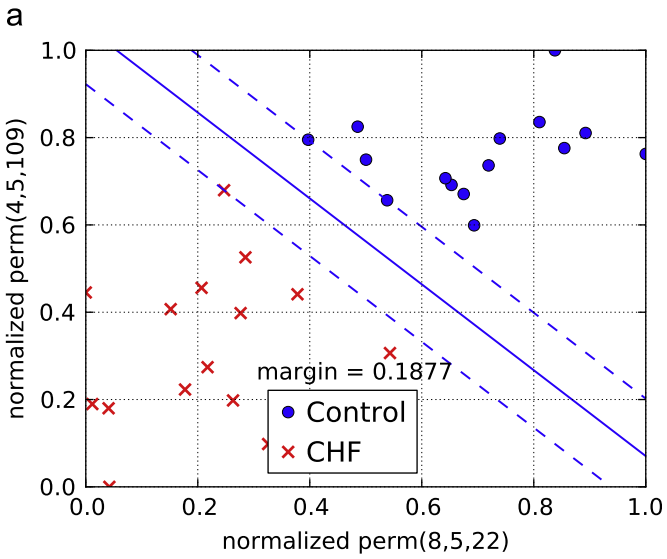

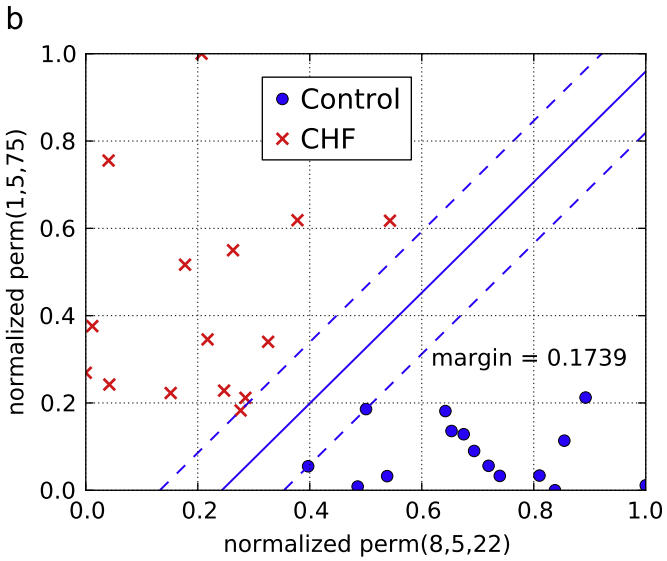

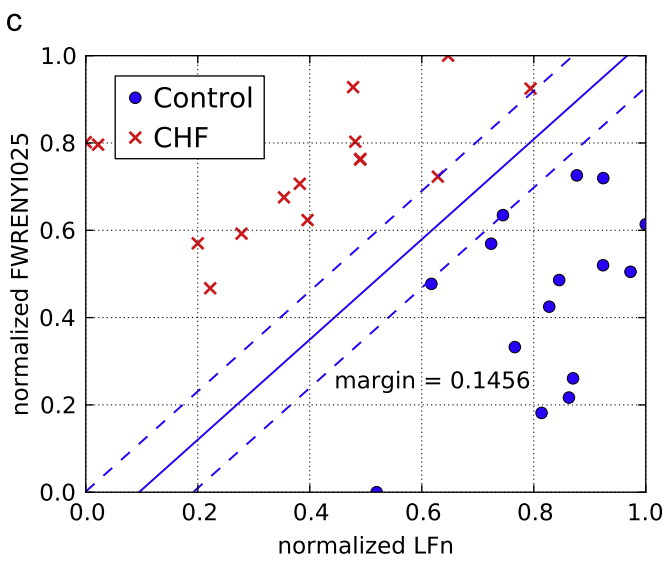

Fig. 7. Distribution of CHF cases (red crosses) and healthy subjects (blue filled circles) in two-dimensional feature spaces. The separating (solid) lines are computed using a linear support vector machine maximizing the margins (indicated by dashed lines). (a) perm(4,5,109) vs. perm(8,5,22), (b) perm(1,5,75) vs. perm(8,5,22), and (c) FWRENYI025 vs. LFn. (For interpretation of the references to color in this figure legend, the reader is referred to the web version of this article.)

clear linear separations of beat-to-beat time series from CHF patients and from the control group.

4. Conclusion

In this article probabilities of ordinal patterns on different time scales were introduced and applied as features for BBI time series classification. Comparison of these features with features based on symbolic dynamics and conventional heart rate variability parameters shows that they provide valuable, non-redundant information about the underlying time series. The discriminative power of the investigated features was quantified in terms of p-values as well as leave-one-out cross validation errors. By using ordinal patterns on different time scales (Fig. 3) (i.e. including lags similar to delay embedding) we obtain maximal descriptive power of most ordinal patterns in a frequency range around 0.1 Hz which is characteristic for the HRV parameter LF (Table 1). This observation is in very good agreement with the fact that CHF is typically associated with reduced low-frequency activity (i.e. small LF values) [32,33].

As a first step towards multi-dimensional classification schemes pairs of features were investigated with respect to their ability to separate the two sets of BBI time series (CHF and control group) with very encouraging results. Therefore, we conjecture that ordinal patterns and symbolic dynamics combined with other HRV parameters in some high dimensional feature space may significantly improve classification results in many applications of beat-to-beat intervals and other cardiovascular time series analysis.

Although, these results are quite encouraging, further applications to similar (and larger) data sets and time series from standardized autonomic tests (hand grip, tilt table, ...) are necessary to obtain a physiological interpretation of ordinal patterns and to evaluate their full power as new biomarker for cardiac data and other (biomedical) time series.

Conflict of interest statement

None declared.

Acknowledgment

The research leading to the results has received funding from the European Community's Seventh Framework Programme FP7/20072013 under Grant agreement 17 No. HEALTH-F2-2009-241526, EUTrigTreat. S.L. acknowledges support from the BMBF (FKZ 01EZ0905/6).

J.K. and N.W. acknowledge support from the Deutsche Forschungsgemeinschaft (KU 837/20-1, KU-837/29-2), from the Federal Ministry of Economics and Technology (FKZ KF2248001FR9) as well as the European projects EU NEST-pathfinder and BRACCIA.

Appendix

The following Python and MATLAB (The MathWorks, Inc.) functions `perm_indices` compute the sequence `indcs` of permutation indices from a time series `ts` for a given word length `wl` and a given lag `lag`.

Listing 1. Python function perm_indices for computing permutation indices.

```
import numpy as np
def perm_indices(ts, wl=4, lag=1):
    m = len(ts)-(wl-1)*lag
    indcs = np.zeros(m, dtype=int)
    for i in xrange(1,wl):
        st = ts[(i-1)*lag : m+((i-1)*lag)]
        for j in xrange(i,wl):
            indcs += st > ts[j*lag : m+j*lag]
        indcs*= wl-i
    return indcs + 1
```

Listing 2. Matlab^{TM} function perm_indices.m for computing permutation indices.

```
function indcs = perm_indices(ts, wl, lag) ;
m = length(ts)-(wl-1)*lag;
 indcs = zeros(m,1) ;
for i = 1:wl-1 ;
  st = ts(1+(i-1)*lag : m+(i-1)*lag) ;
  for j = i:wl-1 ;
    indcs = indcs+(st > ts(1+j*lag : m+j*lag));
  end
  indcs = indcs*(wl-i) ;
end
indcs=indcs + 1 ;
```

References

[1] Task Force of the European Society of Cardiology and the North American Society of Pacing and Electrophysiology, Heart rate variability, European Heart Journal 17 (1996) 354–381.
[2] N. Wessel, A. Voss, J. Kurths, P. Saparin, A. Witt, H.J. Kleiner, R. Dietz, Renormalised entropy: a new method of non-linear dynamics for the analysis of heart rate variability, Comput. Cardiol. 21 (1994) 137–140.
[3] N. Wessel, A. Voss, H. Malberg, Ch. Ziehmann, H.U. Voss, A. Schirdewan, U. Meyerfeldt, J. Kurths, Nonlinear analysis of complex phenomena in cardiological data, Herzschr. Elektrophys. 11 (3) (2000) 159–173.
[4] N. Wessel, H. Malberg, R. Bauernschmitt, J. Kurths, Nonlinear methods of cardiovascular physics and their clinical applicability, Int. J. Bif. Chaos 17 (1) (2007) 3325–3371.
[5] J. Kurths, A. Voss, P. Saparin, A. Witt, H.J. Kleiner, N. Wessel, Quantitative analysis of heart rate variability, Chaos 5 (1) (1995) 88–94.
[6] N. Wessel, C. Ziehmann, J. Kurths, U. Meyerfeldt, A. Schirdewan, A Voss, Short-term forecasting of life-threatening cardiac arrhythmias based on symbolic dynamics, Phys. Rev. E. 61 (1) (2000) 733–739.
[7] D. Cysarz, S. Lange, P.F. Matthiessen, P. van Leeuwen, Regular heartbeat dynamics are associated with cardiac health, Am. J. Physiol. Regul. Integr. Comp. Physiol. 292 (2007) R368–R372.
[8] A. Porta, et al., Entropy, entropy rate, and pattern classification as tools to typify complexity in short heart period variability series', IEEE Transactions on Biomedical Engineering 48 (2001) 1282–1291.
[9] A. Porta, et al., An integrated approach based on uniform quantization for the evaluation of complexity of short-term heart period variability: application to 24 h Holter recordings in healthy and heart failure humans, Chaos 17 (2007) 015117.
[10] A. Voss, J. Kurths, H.J. Kleiner, A. Witt, N. Wessel, P. Saparin, K.J. Osterziel, R. Schurath, R. Dietz, The application of methods of non-linear dynamics for the improved and predictive recognition of patients threatened by sudden cardiac death, Cardiovasc. Res. 31 (1996) 419–433.
[11] S. Akselrod, D. Gordon, F.A. Ubel, D.C. Shannon, A.C. Barger, R.J. Cohen, Power spectrum analysis of heart rate fluctuation: a quantitative probe of beat-to-beat cardiovascular control, Science 213 (1981) 220–222.
[12] A. Malliani, M. Pagani, F. Lombardi, S. Cerutti, Cardiovascular neural regulation explored in the frequency domain, Circulation 84 (1991) 482–492.
[13] J.M. Amigo, Permutation Complexity in Dynamical Systems, Springer Series in Synergetics, Springer-Verlag, Berlin, Heidelberg, 2010.
[14] C. Bandt, B. Pompe, Permutation entropy—a complexity measure for time series, Phys. Rev. Lett. 88 (2002) 174102.
[15] C. Bandt, F. Shiha, Order patterns in time series, J. Time Ser. Anal. 28 (2007) 646–665.
[16] A. Groth, Visualization of coupling in time series by order recurrence plots, Phys. Rev. E 72 (2005) 046220.
[17] M. Staniek, K. Lehnertz, Symbolic Transfer Entropy, Phys. Rev. Lett. 100 (2008) 158101.
[18] J.M. Amigo, S. Zambrano, M.A.F. Sanjuan, True and false forbidden patterns in deterministic and random dynamics, Europhys. Lett. 79 (2007) 50001.
[19] J.M. Amigo, S. Zambrano, M.A.F. Sanjuan, Combinatorial detection of determinism in noisy time series, Europhys. Lett. 83 (2008) 60005.

[20] Y. Cao, W. Tung, J.B. Gao, V.A. Protopopescu, L.M. Hively, Detecting dynamical changes in time series using the permutation entropy, Phys. Rev. E 70 (2004) 046217.
[21] U. Parlitz, S. Berg, S. Luther, A. Schirdewan, J. Kurths, N. Wessel, Classifying cardiac biosignals using order pattern statistics and symbolic dynamics, Proceedings of the Sixth ESGCO 2010, vol. P030, 2010, pp. 1–4.
[22] S. Berg, S. Luther, S.E. Lehnart, K. Hellenkamp, R. Bauernschmitt, J. Kurths, N. Wessel, U. Parlitz, Comparison of features characterizing beat-to-beat time series, Proceedings of the International Biosignal Processing Conference, Berlin, Germany, vol. 49, 2010, pp. 1–4.
[23] B. Frank, B. Pompe, U. Schneider, D. Hoyer, Permutation entropy improves fetal behavioural state classification based on heart rate analysis from biomagnetic recordings in near term fetuses, Med. Biol. Eng. Comput. 44 (2006) 179–187.
[24] http://c.snippets.org/snip_lister.php?fname=perm_idx.c.
[25] N. Wessel, A. Schirdewan, J. Kurths, Intermittently decreased beat-to-beat variability in congestive heart failure, Phys. Rev. Lett. 91 (2003) 119801.
[26] A.L. Goldberger, L.A. Amaral, L. Glass, J.M. Hausdorff, P.C. Ivanov, R.G. Mark, J.E. Mietus, G.B. Moody, C.K. Peng, H.E. Stanley, PhysioBanka PhysioToolkit, and PhysioNet, Circulation 101 (2000) E215.
[27] M.J. Schervish, P values: what they are and what they are not, The Am. Stat. 50 (3) (1996) 203–206.
[28] D.R. Murray, What is "heart rate variability" and is it blunted by tumor necrosis factor?, Chest 123 (2003) 664–667.
[29] S. Guzzetti, R. Magatelli, E. Borroni, et al., Heart rate variability in chronic heart failure, Auton. Neurosci. 90 (2001) 102–105.
[30] M.R. Bristow, R. Ginsberg, W. Minobe, et al., Decreased catecholamine sensitivity and β-adrenergic receptor density in failing human hearts, N. Engl. J. Med. 307 (1982) 205–211.
[31] S. Sonnenburg, G. Raetsch, S. Henschel, C. Widmer, J. Behr, A. Zien, F. de Bona, A. Binder, C. Gehl, V. Franc, The SHOGUN machine learning toolbox, J. Mach. Learn. Res. 11 (2010) 1799–1802.
[32] N. Montano, A. Porta, C. Cogliati, G. Costantino, E. Tobaldini, K.R. Casali, F. Iellamo, Heart rate variability explored in the frequency domain: a tool to investigate the link between heart and behavior, Neurosci. Biobehav. Rev. 33 (2009) 71–80.
[33] S. Guzzetti, R. Magatelli, E. Borroni, S. Mezzetti, Heart rate variability in chronic heart failure, Auton. Neurosci. 90 (2001) 102–105.